Mice deficient for CD137 ligand are predisposed to develop germinal center–derived B-cell lymphoma

Sabine Middendorp,[1] *Yanling Xiao,[1] *Ji-Ying Song,[2] †Victor Peperzak,[1] †Peter H. L. Krijger,[1] Heinz Jacobs,[1] and Jannie Borst[1]

[1]Division of Immunology and [2]Laboratory of Experimental Animal Pathology, The Netherlands Cancer Institute, Amsterdam, The Netherlands

In the germinal center (GC), B cells proliferate dramatically and diversify their immunoglobulin genes, which increases the risk of malignant transformation. The GC B-cell reaction relies on crosstalk with follicular dendritic cells (FDCs), to which the costimulatory receptor CD137 on FDCs and its ligand on GC B cells potentially contribute. We report that mice deficient for CD137 ligand (CD137L) are predisposed to develop B-cell lymphoma, with an incidence of approximately 60% at 12 months of age. Lymphoma membrane markers were characteristic of GC B cells. Longitudinal histologic analysis identified the GC as site of oncogenic transformation and classified 85% of the malignancies found in approximately 200 mice as GC-derived B-cell lymphoma. To delineate the mechanism underlying lymphomagenesis, gene expression profiles of wild-type and CD137L-deficient GC B cells were compared. CD137L deficiency was associated with enhanced expression of a limited gene set that included Bcl-10 and the GC response regulators Bcl-6, Spi-B, Elf-1, Bach2, and activation-induced cytidine deaminase. Among these are proto-oncogenes that mediate GC B-cell lymphoma development in humans. We conclude that CD137L ordinarily regulates the GC B-cell response and thereby acts as a tumor suppressor. (Blood. 2009;114:2280-2289)

Introduction

During the germinal center (GC) reaction, B cells undergo antigen-driven clonal expansion, as well as somatic hypermutation (SHM) and class-switch recombination (CSR) of immunoglobulin (Ig) genes.[1] As a result, memory B cells and plasma cells are formed that provide defense against infectious agents. However, the GC response comes with a risk because SHM and CSR generate DNA breaks, which can lead to chromosomal translocations.[2] These translocations may place proto-oncogenes under control of the active Ig locus and consequently deregulate their expression.[3]

Approximately 95% of newly diagnosed human lymphomas are of B-cell origin; the rest are T-cell malignancies.[3] Because B cells and not T cells undergo antigen receptor gene diversification by SHM and CSR, these statistics clearly indicate the added risk of these GC-specific processes for malignant transformation. GC-derived lymphomas are the most common type of B-cell non-Hodgkin lymphoma in humans and comprise a heterogeneous group of malignancies.[3] A well-characterized GC/B cell–derived malignancy in human is follicular lymphoma (FL), which is defined as a nodular lymphoma with a follicular growth pattern. The lymphoma cells morphologically and phenotypically resemble GC B cells. FL is associated with a t(14;18) translocation that fuses *bcl-2* and *IgH* genes and leads to overexpression of the antiapoptotic protein Bcl-2.[4] GC B-cells normally down-regulate Bcl-2 and are highly prone to apoptosis, which is required to select B-cell clones with a functional and high-affinity membrane Ig (B-cell antigen receptor [BCR]).[5] Apoptosis resistance is therefore an evident mechanism to promote the malignant transformation of these cells.

FL usually runs an indolent course but can progress to an aggressive and rapidly fatal disease in the form of diffuse large B-cell lymphoma (DLBCL). It has been hypothesized that FL pathogenesis not only relies on intrinsic characteristics of the B cell at risk, such as the acquisition of secondary oncogenic mutations, but also on interactions with the microenvironment.[6,7] Whether the disease follows an aggressive or indolent course may be determined by deregulation of the crosstalk between transformed B cells and FDC and T cells in the GC.[6] This hypothesis is derived from genome-wide expression profiling. In the datasets from independent groups that performed such analysis, gene signatures pointing to differential involvement of activated T cells, macrophages, and FDC were part of the prognosis profile.[6-9] Also in DLBCL, gene expression profiling has allowed classification on the basis of both tumor cell intrinsic and environmental information.[8,10]

A GC consists of a framework of FDCs and activated B and T lymphocytes that are mutually dependent. Development of the FDC network requires B cells, whereas FDCs and T cells support the GC B-cell response.[11,12] FDCs retain antigen-antibody complexes on their surface, which interact with membrane Ig on the B cell and thereby provide the primary signal for B-cell survival, expansion, and selection.[11] In addition, adhesion receptors, cytokines, and various tumor necrosis factor (TNF)/TNF receptor family members play a key role in the GC reaction: Interaction between CD40 ligand on activated T cells and CD40 on GC B cells is critical for GC B-cell survival and differentiation. TNF, lymphotoxin α, lymphotoxin β, B-cell activating factor, and their respective receptors also play a reciprocal role in stimulating both FDC

Submitted March 1, 2009; accepted June 21, 2009. Prepublished online as *Blood* First Edition paper, July 16, 2009; DOI 10.1182/blood-2009-03-208215.

*Y.X. and J.-Y.S. are equal second authors.

†V.P. and P.H.L.K. are equal third authors.

The online version of this article contains a data supplement.

The publication costs of this article were defrayed in part by page charge payment. Therefore, and solely to indicate this fact, this article is hereby marked "advertisement" in accordance with 18 USC section 1734.

network formation and the B-cell response. Finally, CD95 on GC B cells in interaction with CD95L on FDC mediates GC B-cell survival as well as death.[4,12,13]

In this study, we report a previously unsuspected role of TNF family member CD137L in the suppression of GC B-cell lymphomagenesis in the mouse. The CD137 (4-1BB, TNFRSF9) receptor/ligand system is best known for its role in T-cell costimulation. CD137 is acquired by both human and mouse T cells upon their activation and supports survival and memory formation of primed CD8$^+$ T cells.[14,15] CD137 is also found on myeloid cells, including macrophages and DC,[16,17] as well as on FDC,[18,19] which is most relevant for the current study. CD137L is expressed on activated myeloid cells and activated B cells. Receptor and ligand engage in bidirectional communication.[20,21] Although no obvious defects in B-cell responses were observed in receptor- and ligand knockout mice,[14,22] triggering of CD137L promoted B-cell proliferation and antibody production in vitro,[18,20] whereas the triggering of CD137 inhibited T cell–dependent humoral immune responses, either by effects on helper T cells or FDC.[23,24] These data suggest that interactions between CD137 on FDC and its ligand on B cells may regulate the GC B-cell response.

Apart from CD137, CD27 (TNFRSF7) has been implicated in the GC B-cell response. In both mice and humans, B cells acquire CD27 during the GC reaction, and its ligand CD70 is expressed on occasional T and B cells in the GC.[25,26] In humans, B cells retain CD27 after the GC reaction and, hence, CD27 is widely used as a marker of memory B cells and GC-derived B-cell malignancies.[25] In the mouse, CD27/CD70 interactions promote B-cell expansion in the GC but do not affect SHM, CSR, or ultimate Ig production.[26] Their role in the GC B-cell response may be more pronounced in humans because of the more abundant expression of CD27 on GC B cells.[25,26]

We present here that mice deficient for CD137L are strongly predisposed to develop GC-derived B-cell malignancies. Most of these were categorized as FL according to the "Bethesda proposals for classification of lymphoid neoplasms in mice,"[27] but they were histologically distinct from human FL. CD27 deficiency did not alter the risk of lymphoma development. On the basis of comparative genome-wide expression profiling of normal GC B cells from wild-type (WT) and CD137L-deficient mice, we have delineated a contribution of CD137L to the GC reaction and thereby identified this molecule as a tumor suppressor.

Methods

Mice

Mice were bred in the animal facility of The Netherlands Cancer Institute under specific pathogen–free conditions, and animal experiments were approved by the Experimental Animal Committee of the Netherlands Cancer Institute and conformed to national guidelines. C57BL/6 (WT), CD27$^{-/-}$, CD137L$^{-/-}$, and CD27;CD137L$^{-/-}$ double-deficient mice were generated and phenotyped by polymerase chain reaction (PCR) as described.[22,28,29] The mice had been backcrossed for 8 to 10 generations to a C57BL/6 background.

Pathology

Mice ranging from 6 to 16 months of age were killed at specific time points. Conventional histopathology was performed on hematoxylin and eosin–stained sections prepared from lymph nodes (including Peyer patches), spleen, thymus, bone marrow, lung, liver, and kidney that were fixed in ethanol-acetic acid-formol saline fixative (40:5:10:45 vol/vol)[30] and embedded in paraffin. Sections were examined blindly for indications of lymphoma according to the Bethesda proposals.[27] The sections were reviewed with a Zeiss Axioskop2 Plus microscope (Carl Zeiss Microscopy) equipped with Plan-Apochroma (5×/0.16, 10×/0.45, 20×/0.60, and 40×/0.95) and Plan Neofluar (2.5×/0.075) objectives. Images were captured with a Zeiss AxioCam HRc digital camera and processed with AxioVision 4 software (both from Carl Zeiss Vision).

Immunohistochemistry

Ethanol-acetic acid-formol saline fixative–fixed, paraffin-embedded tissue of spleen and lymph nodes was sectioned and deparaffinized. Endogenous peroxidase activity was blocked by incubation with 3% H_2O_2 in methanol. Immunohistochemistry was performed for CD3 (clone SP7; Neomarkers), B220 (clone RA3-6B2; BD), and milk fat globule–EGF factor 8 (MFG-E8; clone 18A2-G10; MBL Medical Biological Laboratories Co). Antigen retrieval was obtained for B220, CD3, and MFG-E8 by incubation in 0.1 mol/L citrate buffer, pH 6, for 30 minutes at 95°C, followed by cooling to room temperature for 1 hour. Sections were blocked in phosphate-buffered saline (PBS) with 4% bovine serum albumin (BSA), 5% normal serum, and incubated with primary and secondary antibodies in PBS, 1% BSA, and 1.25% normal serum. Biotinylated goat-derived secondary antibodies were detected by the avidin-biotin-horseradish peroxidase complex method (Dako Systems) by the use of 3,3-diaminobenzidine-tetrahydrochloride (Sigma-Aldrich) as a substrate. For staining with peanut agglutinin (PNA), sections were incubated with biotin-conjugated PNA (Vector Laboratories), which was detected by the avidin-biotin complex method. Sections were counterstained with hematoxylin.

Clonality assay and analysis of SHM

Genomic DNA was isolated from WT spleen and from tumor material derived from aged (CD27)CD137L$^{-/-}$ mice with late-stage disease by proteinase K treatment and ethanol precipitation. The rearranged *JH* genes were amplified by PCR with a set of forward primers to detect most VH gene families[31] and a single reverse primer CTCCACCAGACCTCTCTAGACA that binds within the *JH4* intronic region. PCR products were resolved by agarose gel electrophoresis and visualized by ethidium bromide staining. PCR products were purified from gel by use of the QIAGEN Gel Extraction Kit and sequenced directly on a 3730 DNA analyzer (Applied Biosystems). *JH* intronic nucleotide sequences were compared with sequences from the National Center for Biotechnology Information database (http://ncbi.nlm.nih.gov/genome/seq/BlastGen/BlastGen.cgi.?taxid=10090).

Flow cytometry

Spleens or tumor-cell suspensions were forced through a nylon mesh in Iscove modified Dulbecco medium with 8% fetal calf serum. Erythrocytes were lysed in 0.14 mol/L NH_4Cl and 0.017 mol/L Tris-HCl, pH 7.2. Cells were incubated with Fc Block (2.4G2, BD PharMingen), washed in staining buffer (PBS, 0.5% BSA, 0.01% sodium azide), stained with fluorochrome-conjugated antibodies as indicated, and analyzed with the use of a FACSCalibur (BD) in conjunction with FlowJo software (TreeStar). Monoclonal antibodies (mAbs) used were anti-CD45R/B220 mAb RA3-6B2, anti-CD19 mAb 1D3, anti-CD27 mAb LG.3A10, anti-CD70 mAb FR70, anti-CD86 mAb B7-2, and anti-GL7 mAb GL7 (from BD Biosciences, eBioscience, or purified from available hybridomas). Goat anti–mouse IgM was from Southern Biotech.

Confocal laser scanning microscopy (CLSM)

Small pieces of spleens used for the microarray experiments were embedded in Tissue-Tek OCT compound (Sakura), frozen in dry ice/ethanol, and stored at −80°C. Frozen 5-μm cryostat sections were air-dried overnight, fixed in acetone for 10 minutes, and dried for 1 hour. Sections were rehydrated in PBS and preincubated for 1 hour at room temperature with 2.4G2 mAb to block Fc receptors for Ig. CD137L was detected by purified mAb TKS-1 (BD Biosciences), followed by Alexa 568–conjugated anti-rat Ig. Sections were incubated overnight at 4°C in a humid chamber with allophycocyanin-conjugated B220 mAb (RA3-6B2, BD) and biotinylated anti-FDC mAb (FDC-M2; eBioscience), followed by fluorescein

isothiocyanate–conjugated streptavidin. All antibody incubations were performed in PBS, 0.5% BSA, and 0.02% sodium azide. Slides were mounted in Vectashield (Vector Laboratories) and analyzed with a Leica TCS NT confocal laser-scanning microscope (Leica Microsystems).

GC B-cell isolation, RNA isolation, and amplification

WT and CD137L$^{-/-}$ mice of 8 to 12 weeks were immunized intraperitoneally with 50 μg of chicken γ-globulin conjugated to 4-hydroxy-3-nitrophenylacetyl (NP-CG) in alum or infected intranasally with 25 hemagglutinin units of influenza virus strain A/NT/60/68 (Department of Virology, Erasmus MC Rotterdam) in 50 μL Hanks balanced salt solution. At 9 days after immunization or infection, B cells were enriched from pooled spleens and lymph nodes of 4 mice per test group by magnetic labeled bead cell separation (magnetic-activated cell sorting) with anti–mouse BD Imag CD45R/B220-particles DM, according to the manufacturer's protocol (BD). The B220^{+} magnetic-activated cell-sorted populations were stained with anti–GL7-FITC and anti-CD19-PE to sort CD19^{+}GL7^{+} GC and CD19^{+}GL7^{-} non-GC B lymphocytes by flow cytometry in the presence of propidium iodide on a FACSAria (BD). Sorted GC B cells and non-GC B cells derived from 4 individual mice per test group were pooled, and RNA was isolated by use of the RNeasy kit (QIAGEN). Isolated total RNA was subsequently DNase-treated by use of the QIAGEN RNase-free DNase kit and dissolved in RNase-free H_2O. cDNA was generated by Superscript II reverse transcriptase with total RNA as the template and an oligo(dT) primer containing a T7 polymerase recognition site. Amplified RNA was generated by in vitro transcription by the use of a T7 RNA polymerase (Megascript T7 kit; Ambion).

Gene expression profiling

Microarrays spotted with the Operon v3 oligonucleotide library, covering 20 312 different mouse genes according to the ENSEMBL database were obtained from the central microarray facility of The Netherlands Cancer Institute. Amplified RNA was labeled with the use of Cy5- and Cy3-ULS (ULS aRNA Fluorescent labeling kit; Kreatech) and fragmented into stretches of 60 to 200 bases (RNA fragmentation reagents, Ambion) before the probes were added to the microarray slides. Microarrays were scanned on an Agilent microarray scanner (Agilent Technologies), and data extraction was performed with Imagene 6.0 (BioDiscovery Inc). One experiment was performed by immunization with NP-CG, and 1 experiment was performed by infection with influenza, each with 4 mice per test group. For each microarray analysis, a dye reversal was performed, thus reducing systemic errors caused by oligonucleotide-specific dye preferences. Genes found to be differentially expressed in both experiments, ie, independent of the immunization strategy and with a statistical cutoff ($P < .01$), were classified as being differentially expressed between samples from WT and CD137L$^{-/-}$ mice. Array data have been deposited in ArrayExpress (European Bioinformatics Institute) and are accessible through accession number E-NCMF-29 (http://www.ebi.ac.uk/microarray-as/ae/).

Statistics

For statistical analysis, we used LogXact 7 software (Cytel Inc). *P* values were calculated on the basis of the exact logistic locally weighed polynomial regression.

Results

CD137L-deficient mice are predisposed to develop B-cell lymphoma

Previously, it was shown that CD137L$^{-/-}$ and CD27;CD137L$^{-/-}$ double-deficient mice develop normally and have normal T- and B-cell numbers and subset compositions.[22,28,29] However, at old age, mice of both genotypes became ill at an unusual frequency and were diagnosed with severe neoplasms in spleen and lymph nodes.

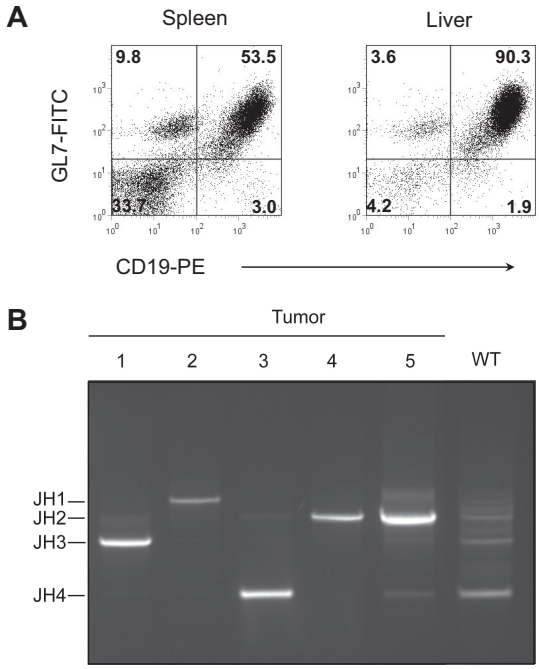

Figure 1. Tumors arising in CD137L$^{-/-}$ mice are B-cell lymphomas of clonal origin. (A) Flow cytometric analysis of tumor cells isolated from spleen and stained for CD19 and GL7 with mAbs directly conjugated to PE or FITC, respectively. Mean fluorescence intensity is represented for each event analyzed. Forward and side scatter gating was set to focus on tumor cells. (B) Diagnosis of tumor clonality by PCR assessing the relative location of rearranged JH1, JH2, JH3, and JH4 segments from V(D)J junctions. Splenic B cells from a WT mouse were used as control for a polyclonal B-cell population. Tumors were in advanced stages and isolated from spleens and liver (case 4) of aged (13-16 months) (CD27$^{-/-}$); CD137L$^{-/-}$ mice. Further characteristics of these tumors are depicted in Table 1.

Flow cytometric analysis revealed that these were of B-cell origin, as hallmarked by expression of CD19, and in most cases expressed the GC B-cell marker GL7 (Figure 1A).[32] The GL7-positive cases also stained strongly with the lectin PNA (PNA^{high}), which is an additional hallmark of GC B cells.[33] Expression of CD27, CD86, and CD70 (data not shown) further supported the notion that the GL7^{+}/PNA^{high} tumors were derived from GC B cells.[25,26] Full-blown tumors that consisted primarily of B cells were diagnosed as clonal by the use of a PCR for *Ig JH* gene segment usage (Figure 1B). In a normal polyclonal B-cell population from WT spleen, PCR products identified multiple rearranged JH gene segments. In contrast, unique PCR products were derived from tumors, denoting a single rearranged *IgH* locus making use of the *JH1*, *JH2*, *JH3*, or *JH4* gene segment (Figure 1B). Nucleotide sequencing of the *VDJ* junctions confirmed clonality (data not shown). Within the set of 5 full-blown B-cell lymphomas depicted, 4 were PNA^{high} (Table 1). In 3 PNA^{high} cases, nucleotide sequencing of the *IgH* locus indicated the occurrence SHM (Table 1). SHM frequency was high compared with what is generally reported for normal GC B cells (see, eg, Delbos et al[31]). The occurrence of SHM further underlined the GC B-cell origin of the GL7^{+}/PNA^{high} lymphomas.

To determine the moment of tumor onset, histologic examination was performed on mice of different age groups ranging from 6 to 16 months. Mice were killed independent of presentation of disease symptoms. In total, 89 CD137L$^{-/-}$ mice and 112 CD27;CD137L$^{-/-}$ mice were examined, whereas 30 WT mice were analyzed for comparison. Spleen, thymus, bone marrow, lung, liver, kidney, and various lymph nodes, including Peyer patches, were processed for sectioning. Sections were examined blindly, and lesions were classified according to defined criteria.[27] The

Table 1. Characteristics of selected late-stage B-cell lymphomas

Lymphoma	CD19	PNA^{high}	IgM	JH gene usage	SHM, no.	SHM percentage
1	+	+	−	JH3	23/691	3.3
2	+	+	−	JH1	18/346	5.2
3	+	+	+	JH4	0/574	0.0
4	+	−	+	JH2	0/502	0.0
5	+	+	+	JH2	42/502	8.4

Lymphomas are identical to those analyzed for JH gene segment usage and clonality in Figure 1. Diagnosis for CD19, PNA, and IgM was performed by flow cytometry. Occurrence of SHM in the Ig locus is stated as number of mutated nucleotides per number of nucleotides sequenced and as percentage calculated from these numbers.

PNA indicates peanut agglutinin; IgM, immunoglobulin M; and SHM, somatic hypermutation.

incidence of lymphoma was plotted as a function of age for mice of each genotype (Figure 2A). Because the number of mice in each age group varied, the incidence of lymphoma showed a rather high variability. To correct for this variability, we also calculated the smoothed estimates (Figure 2B), as based on locally weighed polynomial regression, as specified in "Statistics." This probability model predicts that CD137L deficiency increases the risk of developing FL from 5% to 10% at the age of 7 months to approximately 60% at the age of 12 months and 75% to 90% at the age of 16 months. By using the exact variant of logistic regression, we calculated *P* values to determine statistical significance of each dataset. Both CD137L$^{-/-}$ and CD27;CD137L$^{-/-}$ mice had a significant risk of developing lymphoma ($P < .001$) compared with WT mice, but there was no significant difference in the risk between the 2 knockout mouse strains ($P = .11$). We conclude that CD137L deficiency in mice leads to a significant predisposition to develop B-cell lymphoma, whereas additional CD27 deficiency does not alter this risk.

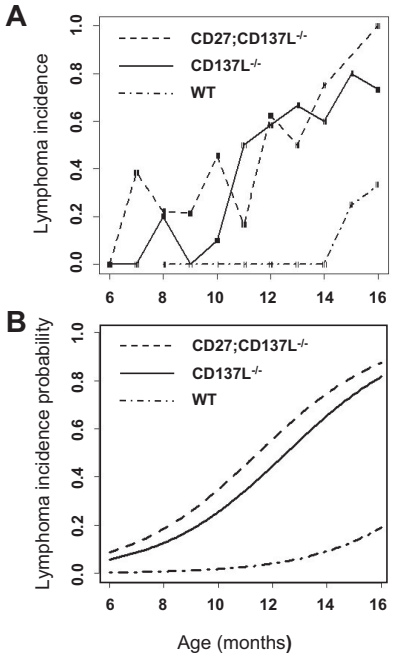

Figure 2. CD137L$^{-/-}$ and CD27;CD137L$^{-/-}$ mice are predisposed to develop B-cell lymphoma. WT, CD137L$^{-/-}$ and CD27;CD137L$^{-/-}$ mice of various ages (6-16 months) were killed and examined blindly for indications of lymphoma according to Bethesda proposals.[27] (A) For each genotype frequencies of lymphoma incidence were determined per age in months. The risk to develop lymphoma was determined on the basis of locally weighed polynomial regression. (B) Trend lines for the smoothed estimates were calculated to determine the lymphoma incidence probability for each genotype. Diagnosis of lymphomas is presented in Table 2.

Lymphoma classification and incidence

Lesions were classified on basis of histology according to the "Bethesda proposals for classification of lymphoid neoplasms in mice."[27] The great majority of the B-cell neoplasias found in our cohort were thus classified as follicular B-cell lymphoma (FL in supplemental Figure 1A, available on the *Blood* website; see the Supplemental Materials links at the top of the online article; and Figure 3A-B). It should be mentioned, however, that mouse FL cannot be considered as the counterpart of human FL because of notable differences in histopathologic features.[27] According to the same classification, cases of small B-cell lymphoma (SBCL in supplemental Figure 1B), DLBCL (supplemental Figure 1C), and anaplastic plasmacytoma (PCT-A in supplemental Figure 1D) occurred at low frequencies.

The results are shown numerically in Table 2. WT mice showed no malignancies before the age of 13 months. In 3 WT mice in the age group of 13 to 16 months, preneoplastic lesions were found, whereas 2 mice presented with FL (14% tumor incidence). This lymphoma incidence (see also Figure 2) in aged WT mice of the C57BL/6 strain is consistent with reported data on lymphoma incidence in aged B6;129 mice.[34] In CD137L$^{-/-}$ and CD27;CD137L$^{-/-}$ mice, preneoplastic disease was frequent in all age groups. Approximately 70% of 13- to 16-month-old mice and approximately 40% of 10- to 12-month-old mice had histologically overt lymphoma. Also in the youngest age group of 6 to 9 months, lymphoma incidence was evident in both strains (7%-17%). The great majority of lymphoma cases concerned early- and late-stage FL, whereas the other lymphoma types occurred in low frequency (Table 2).

Histology reveals tumor progression and defines the GC as site of tumor origin

Histologic examination of CD137L$^{-/-}$ and CD27;CD137L$^{-/-}$ mice revealed a broad spectrum of apparently progressive stages in the development of B-cell neoplasia in spleen, lymph nodes, and Peyer patches and to a lesser extent in thymus and bone marrow. The earliest morphologic changes were related to the B-cell follicles that showed expansion of GCs with thin or absent mantle zones. In the aberrant follicles, increased frequencies of mitotic and apoptotic cells were observed. These were defined as preneoplastic lesions (Figure 4Bii). Progressively confluent nodules were formed by the merging of multiple enlarged GCs that were surrounded by a very thin or no mantle zone, in which centrocyte-like and centroblast-like cells were the major components. This presentation was defined as early-stage FL (Figure 3A). Mitotic and apoptotic rates in these lesions were high. Disease progression was apparent from the simultaneous presence of preneoplastic and early lesions in the same spleen (Figure 3A). For comparison, B-cell follicles in

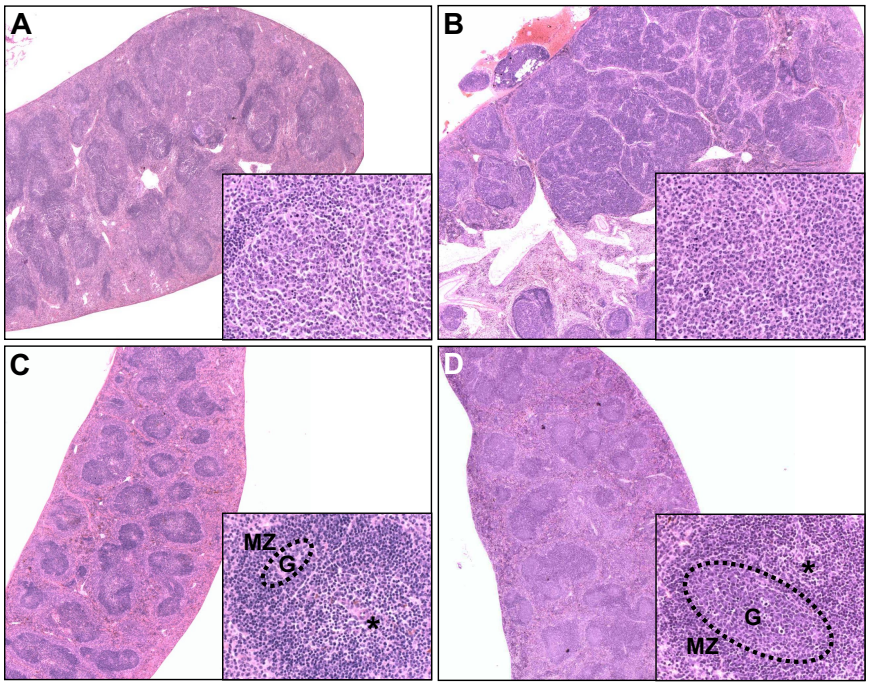

Figure 3. B-cell follicles and their neoplastic transformation. Hematoxylin and eosin–stained spleen sections from (A) a 16-month-old CD137L$^{-/-}$ mouse diagnosed with early-stage FL showing merging of enlarged GCs; (B) an 11-month-old CD27/CD137L$^{-/-}$ mouse diagnosed with late-stage FL showing nodular appearance of tumor mass; (C) a 12-month-old WT mouse, in which the GC (G, dotted circle) is small, and the periarteriolar lymphoid sheath region (*) and mantle zone (MZ) are prominently present, and (D) a 10-week-old WT mouse at day 8 after influenza infection. The GC is enlarged, and the periarteriolar lymphoid sheath region is less pronounced. Original magnifications panels A-D ×2.5, insets ×40.

spleens of a nonimmunized mouse (Figure 3C) and a virus-infected mouse (Figure 3D) are shown.

Further development of the lesions was apparent from their diffuse growth throughout the entire target organ, often with the involvement of liver and kidney. In spleen, the late-stage FL lesions remained more or less nodular (Figure 3B), whereas in lymph nodes and Peyer patches more diffuse patterns were seen (results not shown). The neoplastic cell populations were centrocyte-like and centroblast-like, but transformed blasts resembling immunoblasts and plasmablasts or other large cells with pleomorphism often were present. Also in these lesions, mitotic and apoptotic rates were relatively high (Figure 3B; supplemental Figure 1A).

To examine the GC origin of the lymphomas, we performed immunohistochemistry. Serial spleen and lymph node sections of mice diagnosed with early- and late-stage disease were stained to identify B cells and T cells. This revealed aberrant B-cell follicles in the early-stage disease and large nodular B-cell masses in the late-stage disease, with diminished T-cell zones (Figure 4A). Staining with PNA was performed to specifically detect GC B cells.[33] GC B cells in spleen of a healthy aged WT mouse served as a control (Figure 4Bi). In the mice diagnosed with premalignant lesions, early- and late-stage disease, the histologically aberrant follicles appeared to consist largely of GC B cells (Figure 4Bii-iv).

Immunohistochemistry with an antibody to MFG-E8 was performed to examine whether the aberrant follicles maintained an FDC network. MFG-E8 is identical to the FDC marker FDC-M1 and was previously shown to specifically detect the FDC network in B-cell follicles.[35] In the spleens of nonimmunized, healthy aged WT mice, antibody to MFG-E8 specifically denoted tight FDC networks in B-cell follicles (Figure 5A). It stained the cell body and dendritic processes of the FDCs that were clustered in the GC, adjacent to the mantle zone (Figure 5B). FDC networks became expanded but remained intact in GCs of follicles that were greatly enlarged after infection of 8- to 12-week-old WT mice with influenza virus (Figure 5C-D). In the spleens of mice diagnosed with early-stage FL, FDCs did not form a restricted network as in normal follicles but were more widely dispersed throughout the aberrant follicles (Figure 5E-F). In late-stage FL, FDCs appeared to be sparser and were diffusely distributed throughout the lesions (supplemental Figure 2). Together, these data define the GC as origin of the malignant transformation and strongly suggest a gradual progression from preneoplastic lesions into early- and then late-stage GC-derived B-cell lymphoma.

Table 2. Lymphoma classification and incidence

	CD137L$^{-/-}$			CD27;CD137L$^{-/-}$			WT		
Age, mo	6-9	10-12	13-16	6-9	10-12	13-16	6-9	10-12	13-16
Total, n	28	30	31	53	39	18	6	9	14
Preneoplastic	3	2	1	10	10	3	–	–	3
Early stage FL	1	7	6	4	11	6	–	–	1
Late stage FL	–	5	10	4	5	5	–	–	1
DLBCL	1	–	2	–	–	1	–	–	–
SBCL	–	–	4	1	–	–	–	–	–
PCT-A	–	–	–	–	2	1	–	–	–
Lymphoma incidence, % (no.)	7(2/28)	40(12/30)	71(22/31)	17(9/53)	46(18/39)	72(13/18)	0(0/6)	0(0/9)	14(2/14)

B-cell malignancies observed in CD137L$^{-/-}$, CD27;CD137L$^{-/-}$, and wild-type (WT) mice per age group. Preneoplastic lesions, early- and late-stage GC-derived B-cell lymphoma were defined as outlined in "Results." Classification as follicular lymphoma (FL), diffuse large B-cell lymphoma (DLBCL), small B-cell lymphoma (SBCL), or anaplastic plasmacytoma (PCT-A) was performed according to the Bethesda proposals.[27]

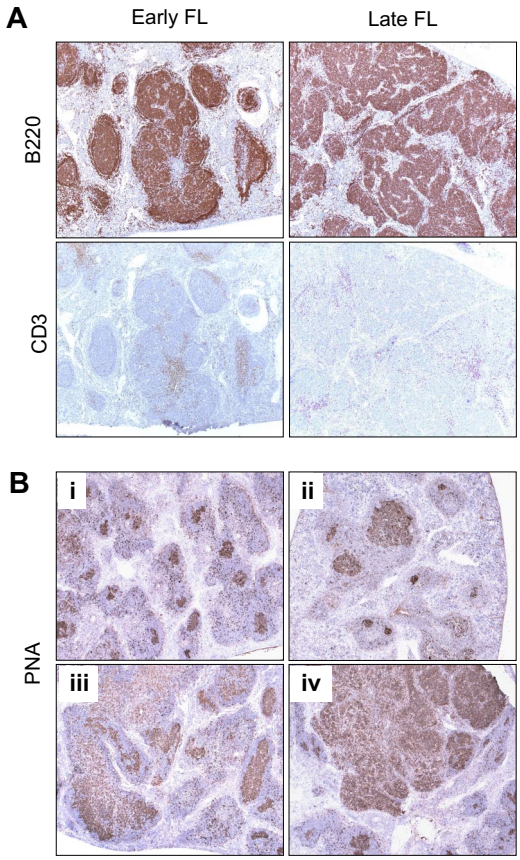

Figure 4. Lymphomas in (CD27;)CD137L$^{-/-}$ mice are of GC B-cell origin. (A) Immunohistochemistry of spleen sections of mice diagnosed with early-stage and late-stage FL by the use of antibody to B220 to detect B cells and antibody to CD3 to detect T cells (serial sections). (B) Histochemistry with PNA was performed to define GC B cells. Shown are spleen sections of mice diagnosed with different stages of FL development: (i) healthy aged WT control, (ii) preneoplastic lesions, (iii) early-stage FL, and (iv) late-stage FL. Original magnification (panels A-B) ×5. Specific staining is shown in brown and hematoxylin counterstaining in blue.

CD137L controls the GC B-cell response

Apparently, CD137L deficiency predisposes mice for malignant transformation of GC B cells, which suggests that CD137L ordinarily reduces the risk of malignant transformation during the GC B-cell response. A potential role for CD137L during the GC reaction is supported by its presence on GC B cells: By using 3-color immunofluorescence analysis of spleen sections from WT and CD137L$^{-/-}$ mice by CLSM, we could specifically detect CD137L expression by those WT B cells that were in close proximity of FDC (Figure 6).

After immunization with NP-CG in alum, we examined GC formation in WT and CD137L$^{-/-}$ mice histologically. No differences were found between these 2 genotypes in terms of numbers or sizes of the GCs or the cellular composition of the GCs, including centrocytic and centroblastic cells, FDCs, and mitotic and apoptotic cells (supplemental Figure 3).

To evaluate the role of CD137L during the GC B-cell response at the molecular level, we performed a comparative genome-wide mRNA expression profiling of WT versus CD137L$^{-/-}$ GC B cells. WT and CD137L$^{-/-}$ mice were immunized with NP-CG in alum (Figure 7; GC1) or were infected intranasally with influenza virus (Figure 7; GC2). Spleen and lymph nodes of 4 mice per genotype were harvested at the peak of the response and were pooled to sort GC B cells by flow cytometry on basis of coexpression of CD19 and GL7. Genes differentially expressed in both datasets, that is, independent of the immunization strategy and with a statistical cut off ($P < .01$), are listed in Figure 7. All genes listed are specific for GC B cells because a concurrent microarray analysis revealed that they were not differentially expressed in CD19^{+}GL7^{-} non-GC B cells from WT and CD137L$^{-/-}$ mice that were sorted alongside with the GC B-cell fraction (Figure 7; non-GC).

The limited number of significant hits thus selected as being overexpressed in CD137L$^{-/-}$ GC B cells included the transcription factors Stat-1, Spi-B, Elf-1, Bcl-6, CIITA, and Bach2; the activation-induced cytidine deaminase (AID), the nuclear factor–κB regulator Bcl-10, as well as the double-strand DNA repair protein Rad21. Interestingly, the majority of these molecules have been implicated in key aspects of the GC B-cell response. Moreover, Bcl-6 and AID are known to drive GC B-cell lymphomagenesis.[37,38] Genes encoding RAG1-activating protein 1 and the DNA mismatch repair protein MLH1 had a lower expression in CD137L$^{-/-}$ GC B cells than in WT GC B cells (Figure 7). These data indicate that CD137L modulates the GC B-cell response by regulating the expression of genes involved in GC-specific processes, including Ig gene diversification. Together, our data strongly support a scenario in which CD137L acts in this way as a suppressor of FL development.

Discussion

We report here that CD137L deficiency predisposes mice to develop GC-derived B-cell lymphoma. Extensive histologic analysis of mice in different stages of tumor development allowed us to unambiguously define GC B cells as the target of malignant transformation in the great majority of cases. By unbiased examination of histologic sections, 64 of 76 malignancies found in the large cohort of mice were classified as GC-derived B-cell lymphoma. This finding was underlined by staining with antibody to the FDC marker MFG-E8 that defined aberrant GC B-cell distribution within an extended and disordered FDC network in early- and late-stage lesions.

Flow cytometric analysis of a limited number of samples indicated the presence of CD27 and its ligand CD70 on these malignant cells (data not shown). From findings in human B-cell malignancies, it has been postulated that CD27/CD70 interactions may support survival and/or expansion of transformed B cells.[25] However, we found that CD27 deficiency did not significantly alter lymphoma incidence in CD137L$^{-/-}$ mice, indicating that CD27/CD70 interactions were not vital to lymphoma development in this setting.

Although the GC-derived B-cell lymphoma that arises in CD137L$^{-/-}$ mice was classified as FL according to the Bethesda proposals, it has an obviously different histologic appearance than human FL. In particular, whereas human FL is indolent, in mouse FL mitotic and apoptotic cells frequently are observed.[27] It is, however, of interest that the expansion of (pre-)malignant B cells in CD137L$^{-/-}$ mice takes place in progressively more disturbed FDC networks. This indicates a follicular growth pattern as observed for human FL. Human FL is associated with t(14;18), leading to Bcl-2 overexpression. In mice, deliberate *bcl-2* overexpression under control of the *IgM* gene enhancer (Eμ) gives rise to follicular hyperplasia but not lymphoma (reviewed in Bende et al[4]). In conjunction with overexpression of the *c-myc* gene, *bcl-2* transgenesis is potently transforming but gives rise to pre–B-cell lymphomas. Also in other contexts, *bcl-2* deregulation or deregulation of other genes instrumental in human B-lymphoma development does not reliably mimic human FL in mice.[4] Possibly, the key genes that

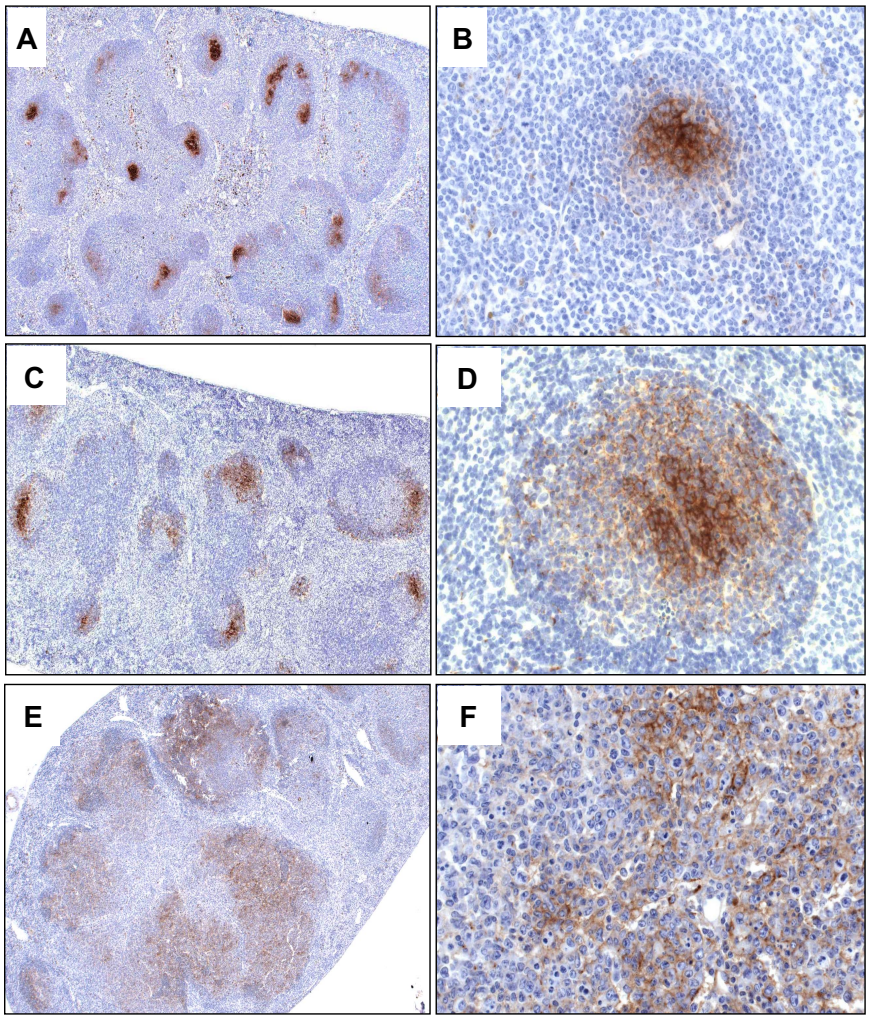

Figure 5. Transformed GC B cells in CD27;CD137L$^{-/-}$ mice expand within a FDC network. Immunohistochemical detection of FDCs with antibody to the marker MFG-E8 in representative spleen sections of a 12-month-old WT mouse (A-B), a 10-week-old mouse at day 8 after infection with influenza virus (C-D), and a representative mouse (n = 5) diagnosed with early-stage FL (E-F). Original magnifications, ×5 (A,C,E); ×40 (B,D,F). Specific staining is shown in brown and hematoxylin and eosin counterstaining in blue.

cooperate with Bcl-2 in human FL development remain to be tested in transgenic mouse models. Alternatively, the GC microenvironment or overall physiology of the mouse is not suitable to generate a model for human FL.

In the present study, we focused on the mechanism that may underlie the malignant transformation of GC B cells in CD137L$^{-/-}$ mice. For this purpose, we have first documented expression of CD137L in the B-cell follicle. CLSM after immunostaining revealed that a selection of follicular B cells express CD137L, namely those that were in close contact with FDC. Specificity of the staining was underlined by its absence in samples from CD137L$^{-/-}$ mice and by evident membrane localization of CD137L (Figure 6). The FDC themselves did not express CD137L, nor did we find any other non-B cells in the follicle that expressed it. CD137 expression on FDC could not be documented because appropriate antibodies to detect mouse CD137 in cryosections are lacking. Therefore, we rely on data from the human system in the supposition that CD137L on GC B cells communicates with

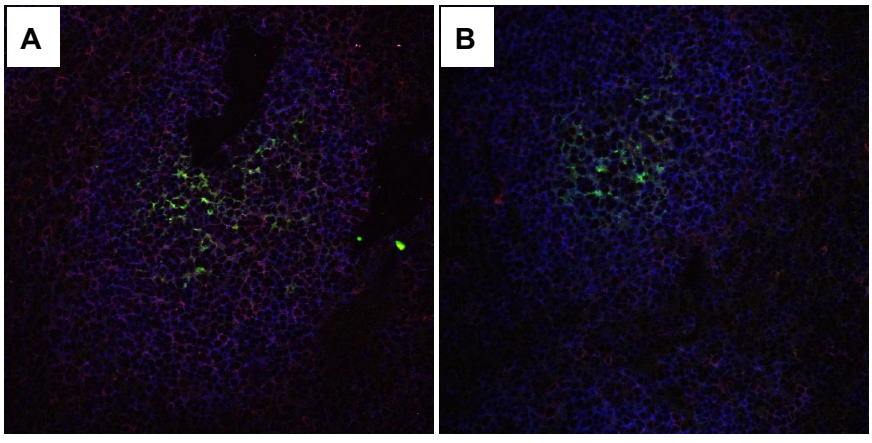

Figure 6. CD137L is expressed on B cells that are in close contact with FDC. CLSM analysis of CD137L expression on B cells and/or FDCs in GC of immunized mice. Cryostat sections of spleens from (A) WT and (B) CD137L$^{-/-}$ mice used for the microarray experiments were stained with mAbs to detect CD137L (red), FDC (FDC-M2[36]; green) and B cells (B220; blue). In the WT sample, B cells that are adjacent to FDC express CD137L, as indicated by the pink color. In the CD137L$^{-/-}$ sample, this signal is virtually absent, indicating specificity of CD137L detection. Original magnification ×40.

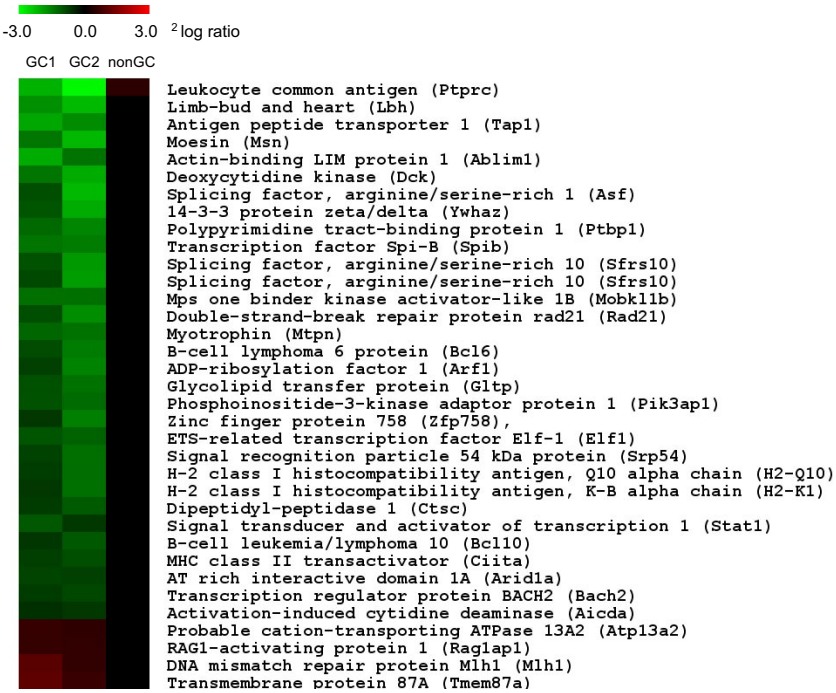

Figure 7. CD137L regulates gene expression in GC B cells. CD19^{+}GL7^{+} GC B cells were sorted by flow cytometry from spleen and lymph nodes of WT and CD137L$^{-/-}$ mice 9 days after immunization with NP-CG (left panel, GC1) or infection with influenza virus (middle panel, GC2). GC B cells of 4 mice per genotype were pooled for each experiment. mRNA was isolated and used for comparative expression analysis by genome-wide microarray. The heat map depicts transcript levels according to the indicated ^{2}log ratio between expression in WT vs CD137$^{-/-}$ GC B cells (see color scale). Green denotes lower expression, and red denotes greater expression in WT GC B cells compared with CD137$^{-/-}$ GC B cells. The list of genes was selected for statistically significant differential expression ($P < .01$) and presence in both experiments. CD19^{+}GL7^{-} non-GC B cells (right panel, nonGC) were sorted simultaneously and analyzed to confirm GC specificity of the listed genes.

CD137 on FDC during the GC reaction. The gene array experiments have provided proof that CD137L plays a specific role during the GC B-cell response. Given the restricted expression pattern of CD137L in the B-cell follicle, we favor the interpretation that CD137L on GC B cells give signals to regulate expression of the genes we have outlined in Figure 7, possibly in response to binding CD137 on FDC. In this scenario, CD137L would act directly as a tumor suppressor in GC B cells.

We have found no differences between 8- to 12-week-old WT and CD137L$^{-/-}$ mice in the histologic appearance of GCs, their overall sizes, and their frequencies of occurrence at day 9 after immunization with NP-CG. Although we cannot exclude differences in GC maintenance for lack of kinetic analysis, we know that WT and CD137L$^{-/-}$ mice produced fully comparable levels of Ig of all isotypes in response to primary and secondary influenza virus infection. Even mice lacking both CD137L and CD27 had normal serum Ig of all isotypes in this setting.[22] However, several data argue for a role of CD137L in regulating the B-cell response. In vitro triggering of CD137L with recombinant CD137 costimulated anti–IgM-induced proliferation of both human and mouse B cells.[18,20] Agonistic antibody to CD137 suppressed T cell–dependent B-cell responses in mice, which was attributed to induction of T-cell anergy[23] but may have involved T cell–dependent attrition of FDC networks.[24] Our study underlines that CD137L plays a role in regulating the GC B-cell response. This role may be compensated for by other factors with regards to eventual Ig production, but we find that it plays a crucial role in suppression of GC B-cell lymphomagenesis. The genes that were found to be down-regulated, either directly or indirectly, by CD137L in GC B cells provide a direct clue as to how such tumor suppression may occur.

The presence of CD137L contributed to down-regulation of AID, which is a key regulator of CSR as well as SHM. AID deaminates cytidines in DNA, which causes DNA strand breaks and activates error-prone DNA repair pathways. These actions lead to the introduction of somatic mutations in *VDJ* recombined *Ig* genes, but the SHM machinery also may target potential oncogenes.[3,4] Accordingly, *AID* deficiency prevented GC-derived B-cell lymphomagenesis in *Bcl-6* transgenic mice.[38] CD137L also contributed to down-regulation of the transcriptional repressor Bcl-6, which is essential for GC formation and affinity maturation[39] and implicated in human GC B-cell lymphomagenesis.[40,41] Bcl-6 negatively regulates p53 expression, thereby allowing GC B cells to sustain the physiologic genotoxic stress associated with high proliferation rate and DNA breaks induced by SHM and CSR.[42] Another major function of Bcl-6 is to inhibit the differentiation of GC B cells into Ig-producing plasma cells. This is mediated by transcriptional repression of the *Blimp1* (*Prdm1*) gene.[43]

CD137L also contributed to down-regulation of the transcription factors Bach2 and Spi-B. Like Bcl-6, these factors attenuate Blimp-1 expression and thereby prevent plasma-cell differentiation, thus sustaining the GC B-cell response.[44-48] Bach2 is required for CSR and SHM[47] and implicated in human B-cell lymphomagenesis.[48] Elf-1, another member of the gene set that is negatively controlled by CD137L is, like Spi-B, a member of the Ets family of transcription factors. It is regulated by the BCR and CD40 and controls *IgH* enhancer elements and potentially CSR.[49] All these findings indicate that CD137L under normal circumstances promotes exit of GC B cells from the GC toward the plasma-cell developmental stage and thereby reduces the risk of malignant transformation in the GC. Down-regulation of Bcl-10, a CARD domain protein that activates nuclear factor κB in response to BCR signaling, also fits in a scenario in which CD137L prevents malignant transformation, in this case by interfering with an essential survival pathway of GC B cells.[50] Several other gene products identified here as potential CD137L targets, such as the DNA repair proteins Rad21 and MHL1, as well as the signal transducer and activator of transcription-1 can be placed in the context of the known literature on the GC reaction, but this becomes more speculative than for the other targets.

On the basis of our findings, we propose that CD137L controls the GC B-cell response by signaling, directly or indirectly, to the GC B cell to down-regulate genes that sustain GC B-cell survival and the GC specific processes SHM and CSR. Thereby, CD137L

promotes exit of the B cells from a hazardous developmental stage and suppresses the risk of transformation.

Acknowledgments

We thank the following coworkers at The Netherlands Cancer Institute: Dr Daphne de Jong for reviewing slides and giving advice on lymphoma diagnosis; Edwi Albering, Joost van Ooij, and personnel of the NKI facilities for animal pathology, flow cytometry, confocal microscopy, microarray, and experimental animal work for expert assistance; and Dr Harm van Tinteren for statistical analysis. We thank Dr Jacques J. Peschon (Amgen) for providing CD137L-deficient mice and Dr Kunihiko Maeda (Yamagata Prefectural University of Health Science) for experimental advice.

This work was supported by grants NKI 2003-2859 and NKI 2004-3087 from the Dutch Cancer Society.

Authorship

Contribution: Y.X. made the initial observation; S.M., Y.X., J.-Y.S., V.P., and P.H.K. designed and performed experiments and analyzed results; H.J. and J.B. designed experiments and analyzed results; and S.M. and J.B. wrote the manuscript.

The current address for Dr Middendorp is the Department of Pediatric Gastroenterology, Erasmus MC, Rotterdam, The Netherlands.

Conflict-of-interest disclosure: The authors declare no competing financial interests.

Correspondence: Jannie Borst, Division of Immunology, The Netherlands Cancer Institute, Plesmanlaan 121, 1066 CX Amsterdam, The Netherlands; e-mail: j.borst@nki.nl.

References

1. Berek C, Berger A, Apel M. Maturation of the immune response in germinal centers. *Cell.* 1991; 67(6):1121-1129.
2. Bross L, Fukita Y, McBlane F, Demolliere C, Rajewsky K, Jacobs H. DNA double-strand breaks in immunoglobulin genes undergoing somatic hypermutation. *Immunity.* 2000;13(5):589-597.
3. Kuppers R. Mechanisms of B-cell lymphoma pathogenesis. *Nat Rev Cancer.* 2005;5(4):251-262.
4. Bende RJ, Smit LA, van Noesel CJ. Molecular pathways in follicular lymphoma. *Leukemia.* 2007;21(1):18-29.
5. Martinez-Valdez H, Guret C, de Bouteiller O, Fugier I, Bachereau J, Liu Y-J. Human germinal center B cells express the apoptosis-inducing genes Fas, c-,myc, p53, and bax but not the survival gene bcl-2. *J Exp Med.* 1996;183(3):971-977.
6. de Jong D. Molecular pathogenesis of follicular lymphoma: a cross talk of genetic and immunologic factors. *J Clin Oncol.* 2005;23(26):6358-6363.
7. Dave SS, Wright G, Tan B, et al. Prediction of survival in follicular lymphoma based on molecular features of tumor-infiltrating immune cells. *N Engl J Med.* 2004;351(21):2159-2169.
8. Staudt LM, Dave S. The biology of human lymphoid malignancies revealed by gene expression profiling. *Adv Immunol.* 2005;87:163-208.
9. Glas AM, Kersten MJ, Delahaye LJMJ, et al. Gene expression profiling in follicular lymphoma to assess clinical aggressiveness and to guide the choice of treatment. *Blood.* 2005;105(1):301-307.
10. Monti S, Savage KJ, Kutok JL, et al. Molecular profiling of diffuse large B-cell lymphoma identifies robust subtypes including one characterized by host inflammatory response. *Blood.* 2005; 105(5):1851-1861.
11. Allen CD, Okada T, Cyster JG. Germinal center organization and cellular dynamics (review). *Immunity.* 2007;27(2):190-202.
12. Park C-S, Choi YS. How do follicular dendritic cells interact intimately with B cells in the germinal center? *Immunology.* 2005;114(1):2-10.
13. Rathmell JC, Townsend SE, Xu JC, Flavell RA, Goodnow CG. Expansion or elimination of B cells in vivo: dual roles for CD40- and Fas (CD95)-ligands modulated by the B cell antigen receptor. *Cell.* 1996;87(2):319-329.
14. Vinay DA, Kwon BS. Role of 4-1BB in immune responses. *Semin Immunol.* 1998;10(6):481-489.
15. Watts TH. TNF/TNFR family members in costimulation of T-cell responses. *Annu Rev Immunol.* 2005;23:23-68.
16. Futagawa T, Akiba H, Kodama T, et al. Expression and function of 4-1BB and 4-1BB ligand on murine dendritic cells. *Int Immunol.* 2002;14(3): 275-286.
17. Schwarz H, Valbracht J, Tuckwell J, von Kempis J, Lotz M. ILA, the human 4-1BB homologue, is inducible in lymphoid and other cell lineages. *Blood.* 1995;85(4):1043-1052.
18. Pauly S, Broll K, Wittmann M, Giegerich G, Schwarz H. CD137 is expressed by follicular dendritic cells and costimulates B lymphocyte activation in germinal centers. *J Leukoc Biol.* 2002;72(1):35-42.
19. Lindstedt M, Johansson-Lindbom B, Borrebaeck CA. Expression of CD137 (4-1BB) on human follicular dendritic cells. *Scand J Immunol.* 2003; 57(4):305-310.
20. Pollok KE, Kim YJ, Hurtado J, Zhou Z, Kim KK, Kwon BS. 4-1BB T-cell antigen binds to mature B cells and macrophages, and costimulates anti-mu-primed splenic B cells. *Eur J Immunol.* 1994; 24(2):367-374.
21. Langstein J, Michel J, Fritsche J, Kreutz M, Andersen R, Schwarz H. CD137 (ILA/4-1BB) a member of the TNF receptor family induces monocyte activation via bidirectional signaling. *J Immunol.* 1998;160(5):2488-2494.
22. Hendriks J, Xiao Y, Rossen JW, et al. During viral infection of the respiratory tract, *CD27,* 4-1BB, and OX40 collectively determine formation of CD8+ memory T cells and their capacity for secondary expansion. *J Immunol.* 2005;175(3):1665-1676.
23. Mittler RS, Bailey TS, Klussman K, Trailsmith MD, Hoffmann MK. Anti-4-1BB monoclonal antibodies abrogate T-cell–dependent humoral immune responses in vivo through the induction of helper T cell anergy. *J Exp Med.* 1999;190(10):1535-1540.
24. Sun Y, Blink SE, Chen JH, Fu YX. Regulation of follicular dendritic cell networks by activated T cells: the role of CD137 signaling. *J Immunol.* 2005;175(2):884-890.
25. Lens SMA, Tesselaar K, van Oers MHJ, van Lier RAW. Control of lymphocyte function through CD27-CD70 interactions. *Semin Immunol.* 1998; 10(6):491-499.
26. Xiao Y, Hendriks J, Langerak P, Jacobs H, Borst J. CD27 is acquired by primed B cells at the centroblast stage and promotes germinal center formation. *J Immunol.* 2004;172(12):7432-7441.
27. Morse HC, Anver MR, Fredrickson TN, et al. Bethesda proposals for classification of lymphoid neoplasms in mice. *Blood.* 2002;100(1):246-258.
28. Hendriks J, Gravestein LA, Tesselaar K, van Lier RA, Schumacher TN, Borst J. CD27 is required for generation and long-term maintenance of T-cell immunity. *Nat Immunol.* 2000;1(5):433-440.
29. DeBenedette MA, Wen T, Bachmann MF, et al. Analysis of 4-1BB ligand (4-1BBL)-deficient mice and of mice lacking both 4-1BBL and CD28 reveals a role for 4-1BBL in skin allograft rejection and in the cytotoxic T-cell response to influenza virus. *J Immunol.* 1999;163(9):4833-4841.
30. Harrison PT. An ethanol-acetic acid-formol saline fixative for routine use with special application to the fixation of non-perfused rat lung. *Lab Anim.* 1984;18(4):325-331.
31. Delbos F, De Smet A, Faili A, Aoufouchi S, Weill JC, Reynaud CA. Contribution of DNA polymerase eta to immunoglobulin gene hypermutation in the mouse. *J Exp Med.* 2005;201(8):1191-1196.
32. Han S, Zheng B, Schatz DG, Spanopoulou E, Kelsoe G. Neoteny in lymphocytes: Rag1 and Rag2 expression in germinal center B cells. *Science.* 1996;274(5295):2094-2097.
33. Rose ML, Birbeck MS, Wallis VJ, Forrester JA, Davies AJ. Peanut lectin binding properties of germinal centres of mouse lymphoid tissue. *Nature.* 1980;284(5754):364-366.
34. Haines DC, Chattopadhyay S, Ward JM. Pathology of aging B6;129 mice. *Toxicol Pathol.* 2001; 29(6):653-661.
35. Kranich J, Krautler NJ, Heinen E, et al. Follicular dendritic cells control engulfment of apoptotic bodies by secreting Mfge8. *J Exp Med.* 2008; 205(6):1293-1302.
36. Taylor PR, Pickering MC, Kosco-Vilbois MH, et al. The follicular dendritic cell restricted epitope, *FDC-M2*, is complement C4; localization of immune complexes in mouse tissues. *Eur J Immunol.* 2002;32(7):1888-1896.
37. Baron BW, Anastasi J, Montag A, et al. The human BCL6 transgene promotes the development of lymphomas in the mouse. *Proc Natl Acad Sci U S A.* 2004;101(39):14198-14203.
38. Pasqualucci L, Bhagat G, Jankovic M, et al. AID is required for germinal center-derived lymphomagenesis. *Nat Genet.* 2008;40(1):108-112.
39. Ye BH, Cattoretti G, Shen Q, et al. The BCL-6 proto-oncogene controls germinal-centre formation and Th2-type inflammation. *Nat Genet.* 1997; 16(2):161-170.
40. Baron BW, Nucifora G, McCabe N, Espinosa R, Le Beau MM, McKeithan TW. Identification of the gene associated with the recurring chromosomal translocations t(3;14)(q27;q32) and t(3;22)(q27; q11) in B-cell lymphomas. *Proc Natl Acad Sci U S A.* 1993;90(11):5262-5266.
41. Lo Coco F, Ye BH, Lista F, et al. Rearrangements

of the BCL6 gene in diffuse large cell non-Hodgkin's lymphoma. *Blood.* 1994;83(7):1757-1759.

42. Phan RT, Dalla-Favera R. The BCL6 proto-oncogene suppresses p53 expression in germinal-centre B cells. *Nature.* 2004;432(7017):635-639.
43. Shaffer AL, Yu X, He Y, Boldrick J, Chan EP, Staudt LM. BCL-6 represses genes that function in lymphocyte differentiation, inflammation, and cell cycle control. *Immunity.* 2000;13(2):199-212.
44. Ochiai K, Muto A, Tanaka H, Takahashi S, Igarashi K. Regulation of the plasma cell transcription factor Blimp-1 gene by Bach2 and Bcl6. *Int Immunol.* 2008;20(3):453-460.
45. Schmidlin H, Diehl SA, Nagasawa M, et al. Spi-B inhibits human plasma cell differentiation by repressing BLIMP1 and XBP-1 expression. *Blood.* 2008;112(5):1804-1812.
46. Su GH, Muthusamy N, Garrett-Sinha LA, Baunoch D, Tenen DG, Simon MC. Defective B-cell receptor-mediated responses in mice lacking the Ets protein, *Spi-B. EMBO J.* 1997;16(23):7118-7129.
47. Muto A, Tashiro S, Nakajima O, et al. The transcriptional programme of antibody class switching involves the repressor Bach2. *Nature.* 2004;429(6991):566-571.
48. Sakane-Ishikawa E, Nakatsuka S, Tomita Y, et al. Prognostic significance of BACH2 expression in diffuse large B-cell lymphoma: a study of the Osaka Lymphoma Study Group. *J Clin Oncol.* 2005;23(31):8012-8017.
49. Grant PA, Andersson T, Neurath MF, et al. A T-cell–controlled molecular pathway regulating the IgH locus: CD40-mediated activation of the IgH 3′ enhancer. *EMBO J.* 1996;15(23):6691-6700.
50. Du MQ, Peng H, Liu H, et al. BCL10 gene mutation in lymphoma. *Blood.* 2000;95(12):3885-3890.